Studies of pulse shapes from semiconductor detectors

Johan Rohlén, Erika Nettö and Julien Millet

Department of Fundamental Physics
Chalmers University of Technology and Göteborg University

Abstract

In subatomic experiments identifying what kind of particles that emerge from different reactions has always been a problem. Usually this identification is done by using ΔE-E detectors or time of flight, however there is another alternative using pulse shape discrimination (PSD) with pulses from semiconducting detectors. The idea behind PSD is that particles will give a different rise time depending on there charge and mass and this dependency is to be used for identification. According to theory a heavy charged particle should give a faster rise time than a light charged particle.

We investigate the underlying theory to understand why the method of using the pulse shape from silicon detectors might work and what kind of electronics that are favourable in collecting data. Different data analysing methods are developed to investigate if the data collected inhibit the dependency that are needed to identify what particle was detected.

We obtained data from two experiments, one in Spain and one in Sweden. The experiment in Spain was made at Centro Nacional de Acceleradores in Seville and in Sweden at Chalmers/Gothenburg University in Gothenburg. In Seville experimental problems were encountered that resulted in the data being inconsistent and difficult to analyse. This lead to that no conclusions could be made from that experiment, however some favourable tendencies can be observed. In Gothenburg there is only possible to use natural radiation sources such as, ^{4}He, fission products and electrons for detection. This limits the ability to compare different types of particles with each other but we can make some simple tests to see if the theory works.

Unfortunately the data that was collected from the experiment in Seville was incorrect. This lead to inconclusive results and no conclusions could be made from that data although some tendencies toward the dependency that we where looking for could be seen. In Gothenburg we only tested ^{4}He and a fission source, but because of the fission products large kinetic energy the electronics had problems generating a good pulse. This lead to that pulses from ^{4}He had faster rise times than the fission products, which is contradictory to what we have predicted. Some scatter plots are made to show how the dependencies that might be, or not be, in the data could look like.

Contents

Chapter 1

Introduction

For fundamental understanding of the principles that govern the subatomic physics one have to make different kinds of experiments that probe the inside of a nucleus. This is usually done by shooting particles on a nucleus and investigating the out coming radiation, charged particles and/or photons. Another way is to investigate what emerges from different radioactive decays. Measuring the energy of the resulting radiation is fairly easy and can be done using different kinds of detectors depending on the kind of radiation. For charged particles, which this thesis deals with, semiconducting detectors are used, which most often are made of silicon.

Whilst the energy of the charged particles is easy to measure it is much more difficult to identify what kind of particle was detected, i.e. if it was a ^{4}He or a ^{6}Li. Traditionally this is done by a telescope setup using $\Delta E - E$ detectors or measuring the time of flight. $\Delta E - E$ detectors consists of one very thin detector where the particles pass through and lose parts of their energy and a thicker detector which stops the particle. Both the energy loss in the thin detector and the energy deposited in the thicker detector is measured and by comparing these, identification of what kind of detected particle can be made, see Figure 1.1. However, this technique fails at lower energies mainly because particles are stopped in the thin detector. To identify low energy particles another method must be applied, and one such method is pulse shape analysis, also known as pulse shape discrimination, PSD.

For a long time it has been known that the rise time of the signal from silicon detectors is dependent of the charge and mass of the incoming, interacting particle. Research in this area have developed a method for PSD, and discrimination of light charged particles was achieved by exploiting the signal rise time from charge-sensitive preamplifier's. This method is comparable and sometimes better than traditional telescope technique with $\Delta E - E$ detectors. [5]

Earlier experiments done to test the PSD method, with totally depleted silicon detectors in reverse mount has been successful according to [5] [6] [8] [9] [10]. It is an excellent method for identification of charged particles, down to $4MeV/u$ (i.e. energy by nucleon) from hydrogen up to fluorine [10]. According to [6], charged particles have been identified in the energy range of $2-20MeV/u$. For energies lower than $2MeV/u$ separation of particles

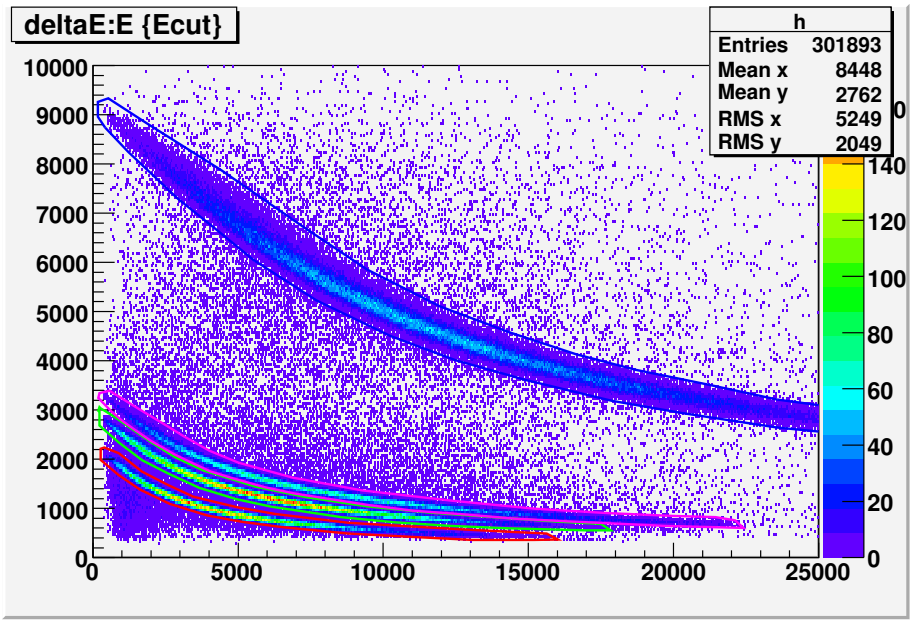

Figure 1.1: Identification of charged particles using $\Delta E - E$ detectors.

is no longer observed and the discrimination fails. It is at energies below this limit we want to investigate and try to separate charged particles by using a modified PSD method.

Chapter 2

Theory

To understand why there is a difference in rise time of the signal from silicon detectors for different charged particles the theory behind the interaction between radiation and matter must be understood. How a silicon detector operates and why it is favourable for identification of charged particles is also discussed.

2.1 Interaction between radiation and matter

To detect radiation there has to be an interaction between the radiation and the detecting material, the absorber. Since there are different types of radiation, and every radiation has its specific type of interaction with matter, different kinds of detectors has been developed.

The radiation types of the left side of the Table 2.1 below interacts with the electrons in the matter by the Coulomb force. The types on the right side on the other hand first have to experience catastrophic interaction, which often involves the atomic nucleus of the matter, that changes the properties of the incoming radiation in a single encounter.

Table 2.1: Different types of radiation and corresponding penetration depth.

Charged Particle Radiations		**Uncharged Radiations**
Heavy charged particles (characteristic length $\cong 10^{-5}m$)	$\Leftarrow$	Neutrons (characteristic length $\cong 10^{-1}m$)
Fast electrons (characteristic length $\cong 10^{-3}m$)	$\Leftarrow$	X-rays and gamma rays (characteristic length $\cong 10^{-1}m$)

In all types of radiation, the interaction transfer energy from the radiation to the absorber. This energy is fully or partly transferred from the incoming radiation to the electrons or nucleus in the detection material or to charged particles as a product of nucleus reactions.

If there is no interaction within the detector the charged radiation passes the detector without leaving any trace of its existence.

The arrows in the table shows what happens at a catastrophic interaction. X-rays and gamma rays transfer their energy to the electrons in the detecting material. This transfer produces secondary electrons, which behaves like fast electrons. Gamma ray detectors are constructed to promote this kind of interaction and then stop the secondary electrons so that all energy can be transferred and to give an output signal. Neutrons interacts in a way that secondary heavy charged particles emerges, which works as a base for the detector signal. The characteristic length is the penetration length (or mean free path) the radiation have in the solid matter.

Heavy charged particles, like α particles, experience Coulomb force between their positive charge and the negative charge of the orbital electrons within the absorber atoms. Interactions of the charged particle with the nucleus of the absorber atoms (like Rutherford scattering for example) are possible but rarely occur. These kinds of interactions are not normally significant in the response of radiation detection.

At the encounter, the heavy charged particles interacts with many electrons in the absorber. These electrons feels an impulse from the attractive Coulomb force which may excite the electrons or ionise the absorber atom.

The maximum energy the charged particles can transfer is $4Em_0/m$, which is about $1/500$ of the total energy of the particle/nucleon, where E is the kinetic energy of the particle, m_0 is the electronic mass and m the mass of the charged particle. During the slowing down process, the charged particle does not greatly deflect from a straight path, except at the end of its track when the velocity is low and, hence, the impulse have a stronger effect of its track.

The products of these encounters in the absorber are excited electrons or ion pairs, which is a free electron and a corresponding positive ion. These pairs naturally recombines, but this process is in some detectors suppressed so that the ion pairs may be used as a basis of the detectors response. In particular close encounters the electrons may obtain large enough impulse that its kinetic energy after leaving its parent atom is enough to ionise again. These electrons are called delta rays. The majority of the energy loss of the charged particle occurs via these delta rays. Since delta rays have a small range the ionisations form closely to the track of the charged particle. Thus, the ions are not formed randomly single spaced but as clusters along the charged particle path.

The stopping power is an important factor and is defined as the differential energy loss within the material divided by the differential path length:

$$S = -\frac{dE}{dx} \tag{2.1}$$

For particles with a given charge state, S increases as the particle velocity decreases. This is described by the Bethe (Bloch) formula [2]:

$$S = -\frac{dE}{dx} = \frac{4\pi e^4 z^2}{m_0 v^2} NB \tag{2.2}$$

where N = number density which is the number of valence electrons per volume, and

$$B = Z\left[ln\frac{2m_0v^2}{I} - ln(1 - \frac{v^2}{c^2}) - \frac{v^2}{c^2}\right] \tag{2.3}$$

which is proportional to Equation (2.4) for non-relativistic values of v.

$$Z\left[ln\frac{2m_0v^2}{I}\right] \tag{2.4}$$

In these expressions, v and ze is the velocity and charge of the incoming charged particle, N and Z are the number density and atomic number of the absorber atom, m_0 is the electronic rest mass and e its charge. I is the average excitation and ionisation potential of the absorber and is normally treated as an experimentally determined parameter for each element.

Formula is valid for charged particles provided their velocity is much greater than the velocity of the absorber electrons. Since B varies slowly with the energy, S varies $\propto 1/v^2$, the inverse kinetic energy. When the charged particle slows down because of the stopping power, it spends a greater time in the vicinity of a given electron which gives that the impulse felt by the electron, and hence the transferred energy, is the largest.

The Bethe formula (Equation (2.2) fails at low particle energy because of charge exchange between the charged particle and the absorber. Then the particle reduces its effective charge and hence also its energy loss. At the end of the track the charged particle has become neutralised and has transferred all of its energy to the absorber.

Figure 2.1 below, shows the differential stopping power versus energy for different charged particles using a program , SRIM, that calculates the stopping power even for lower energies.

A plot of the differential energy loss, dE/dx, versus the track of the particle, along the track is called a Bragg curve. Figure 2.2, [1], shows a typical Bragg curve for particles in matter. Depending on the particle mass and charge the amount of energy transferred by the particle along its path is different for every particle. As the particle travels through the detector it loses energy. At some specific energy the curve falls off because the charged particle starts to pick up electrons. This makes it less charged and hence, according to the Bethe formula, $-dE/dx$ reduces and eventually the particle has become neutralised and at rest, so the curve falls off. [1] [2]

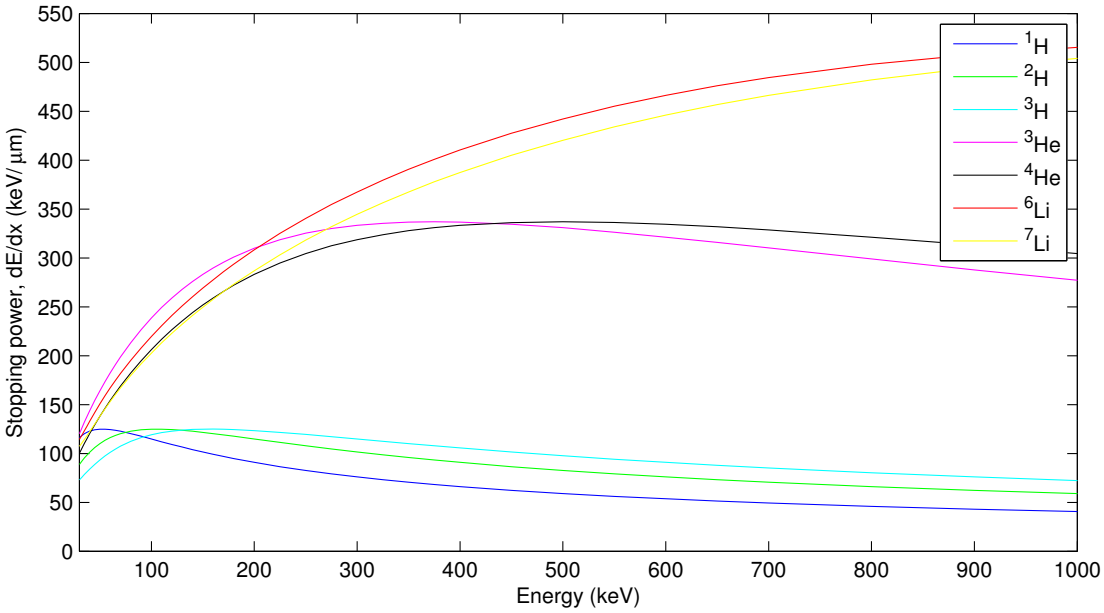

Figure 2.1: Stopping power in silicon for different particles.

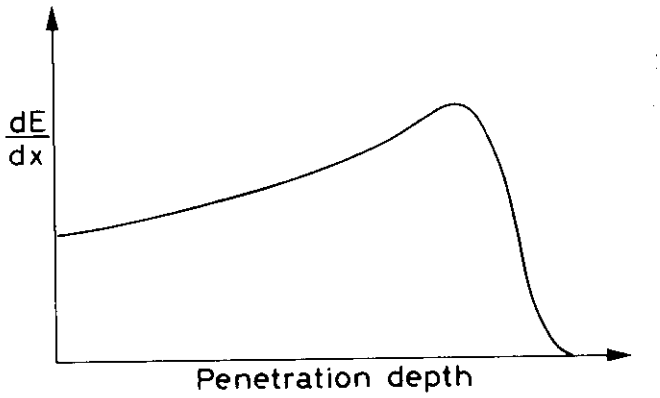

Figure 2.2: Typical Bragg curve showing the variation of dE/dx as a function of the penetration depth of the particle in matter

2.2 Detectors

For radiation to be detected there has to be an interaction between the incoming radiation and the absorber atoms in the detector. When radiation enters and interacts with the atoms it loses energy which releases electrons from their atomic orbits. These electrons are collected and formed into a voltage or current pulse for analysis by electronic circuitry. The material and thickness of the detector must be chosen to what kind of radiation one wants to detect and which information one wants to gather. For α particles from radioactive decay very thin detectors are sufficient, typically less than 100 μm in most solids. For electrons, such as emitted from β decays, solids of 0.1 to 1 mm is required, while for gamma rays a detector of 5 cm may not be sufficient to detect all incoming radiation.

To demonstrate the presence of radiation, a Geiger counter could be used where all kinds of incident radiation gives the same output. To measure the energy of the radiation a detector should be selected that converts the energy of the pulse by an amplitude of the output pulse from the collected electrons. To do this a large number of electrons must be released in the detector so that the statistically fluctuations of electrons, or failure to count a few electrons, does not have a large impact on the determination of the energy. To determined at what time the radiation was emitted a detector is needed that quickly collects the electrons. Here the number of electrons is of less importance. Determination of the particle entering the detector, the mass or charge of the particle must leave its signature in the detector material.

If the intensity of the radiation is high the detector material must be able to quickly recover from one radiation before counting the next. Position detection of a particle requires that the detector must be sensitive to the path of the radiation.
No single detector can measure everything at the same time. Since we are going to do experiments on semiconducting detectors that is what we are focusing on. [3]

2.2.1 Semiconductor detectors

As the name implies semiconducting material, like silicon for example, is used as absorber material in the detectors. Since semiconducting detectors are in solid state at room temperature they are also called solid state detectors. These devices were practically available in the early 1960s and quickly became useful to nuclear physicists because of the high energy resolution in particle detection.

The early versions of semiconducting detectors were called crystal counters. Modern detectors are referred to as semiconductor diode detectors, or simply solid state detectors. Technically, scintillation counters also can be thought of as solid state detectors but it has come into widespread use to characterise only those devices based on electron-hole pair collection from semiconductor media as solid state detectors.

Another advantage is the size of the detector. Since semiconductors are solid at room temperature, and hence are relatively dense, the detectors can be very small. Drawbacks, on the other hand, may include the limitation to small sizes and the relatively high susceptibility of these devices to performance degradation from radiation induced damage.

Silicon and germanium are the two semiconductors that are mainly used for these detectors. Silicon is the most commonly used material in diode detectors made for detection of charged particles while germanium is more widely used for gamma ray measurements. Silicon have several advantages such as that no cooling is needed for operation and it is easy and cheap to manufacture. Germanium however needs to be cooled down to reduce noise and is relatively expensive to manufacture. The main reason why germanium is used at all is that it has a much higher Z which makes interactions with photons much more likely.

Because of the periodic lattice in crystalline materials there are energy bands formed in the solid where the electrons can exist. The energy of any electron within the material must be confined to one of these energy bands, which may be close to each other or separated by gaps. The lower band is called the valence band. This corresponds to the outer shell electrons bounded to specific lattice sites within the crystal. In silicon or germanium the electrons are a part of the covalent bonding that constitute inter atomic forces within the crystal.

The upper band is called the conducting band. Electrons in this band are free to migrate through the crystal and are the ones that contribute to the conductivity of the material.

These two bands are separated by a band gap where there are no allowed energy levels. It is the size of the gap that determines if a material is a metal, a semiconductor or an insulator, illustrated in Figure 2.3, [1]. Semiconducting materials are not insulators nor metals but a middle thing. In metals the valence band is overlapping the conductivity band which makes it easy for electrons to migrate through the material. Metals are therefore characterised by high electrical conductivity and because of this metals are used as media in wires for electrical current to flow.

Semiconductors and insulators on the other hand have a gap between the valence and the conducting band that the electrons must cross. The size of the band gap is determined by the lattice constant, the distance between the atoms in the crystal, and also the temperature and pressure. For semiconductors the gap is about 1 eV while for insulators the gap is larger than 5 eV. For a current to flow the electrons must be excited from the valence to the conductivity band. In insulators current needs application of a strong electric field to flow while in semiconductors electrons sometimes can be excited and a small current can flow. This is why their conductivity is many orders of magnitude lower compared to the metals.

At 0 K all of the electrons contribute to the covalent bindings between the atoms of the crystal, but at any nonzero temperature the electrons share the thermal energy of the crystal and excitation between the bands is possible. At room temperature a few electrons are excited from the valence band to the conduction band by the thermal energy. The disorientation from their lattice sites creates electron hole pairs. If these holes are filled in with electrons nearby, which in their turn leaves a hole, the hole will move and an electrical

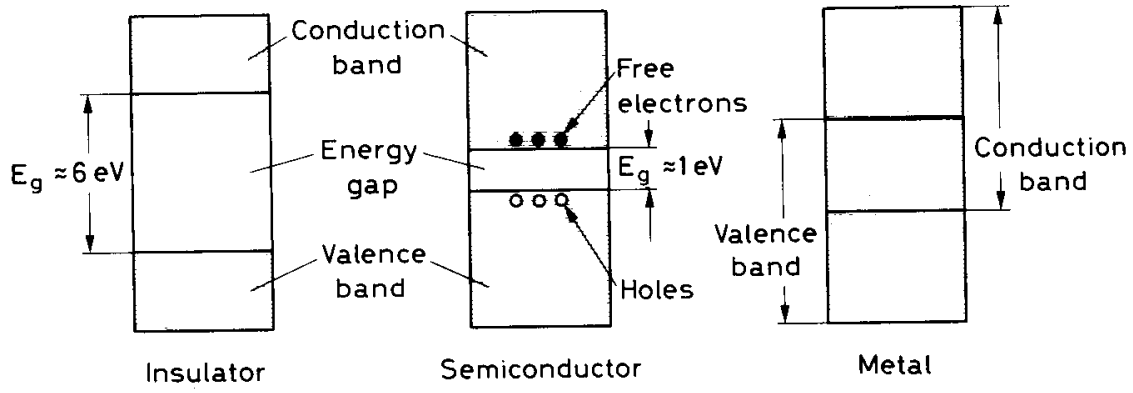

Figure 2.3: Energy bands for insulators, semiconductors and metals

current will flow. When an electrical field is applied the electron and the hole will move in opposite ways. [1] [2]

Certain impurities in the detector affects the conductivity drastically. The addition of one boron atom to 10^5 silicon atoms the conductivity increases by a factor of 10^3 compared to pure silicon. Adding these trace elements to affect the conductivity of an element is called to dope the element. In silicon, every atom has four outer electrons that forms the four covalent bindings between the silicon atoms. The addition of a trace element of valence five, one electron does not contribute to the bindings but is left over and is the reason for the increased conductivity. Impurity atoms that can give up one electron is called a donor because when the atom is ionised it donates an electron to the conduction band and the detector is said to be n-doped because it has extra negative charge.

Adding an element of valence three all four covalent bindings can be formed but there is a electron vacancy, a hole, which contributes also to an increased conductivity. These impurity atoms are called acceptors because they accept electrons from the valence band in order to complete the covalent bonds with neighbour atoms, leaving holes in the band. Detectors with impurities of trace elements with valence three is called p-doped because it lacks electrons and hence is positive. [4]

When a semiconductor is irradiated by neutrons, some neutrons are captured by the detector atoms. If these atoms undergo a nuclear reaction, another atom is formed and the detector has become doped. E.g. if a silicon detector is irradiated with neutrons, some of the silicon atoms will capture a neutron and through a nuclear reaction become a phosphorus atom, and hence the silicon is n-doped. Neutron doping provides a more homogeneously doped detector and the detectors are said to be transmutation doped.

The probability per unit time for an electron to be thermally excited is:

$$p(T) = \frac{CT^3}{2e^{-\frac{E_g}{2kT}}}$$

where T is the absolute temperature, k the Boltzmann constant, E_g the energy band gap and C a proportionality constant.Hence, a high energy gap means low probability for excitation. In absence of a electrical field the electron and hole will eventually recombine. After formation of the pair, the electron and the hole will take part in a random thermal motion which leads to diffusion away from the origin were the pair was created. This diffusion leads to a broadening distribution of the charges as a function of time. A cross section through this distribution would be approximated by a Gaussian function with a standard deviation:

$$\sigma \propto \sqrt{\mu T t}$$

where μ is the mobility of the charge carrier, T is the absolute temperature and t is the elapsed time. The drift velocity of a hole or an electron:

$$v_{hole} = \epsilon \cdot \mu_{hole} \ , \quad v_{electron} = \epsilon \cdot \mu_{electron}$$

where ϵ is the electrical field magnitude. In semiconductors μ_{hole} and $\mu_{electrons}$ are roughly of the same order. For gases $\mu_{electrons} >> \mu_{ions}$

At higher electrical field the drift velocity increases more slowly with the field. Saturation velocity is reached which becomes independent of further increases in the electrical field. Many semiconducting detectors are operated with electrical field values sufficiently high to result in saturated drift velocity for charge carriers over typical dimensions of $0,1\ cm$ will be under $10\ ns$. This makes semiconductor detectors among the fastest responding of all radiation detector types.

Because of diffusion there are limits in the precision to which position measurements can be made using the location at which charges are collected at the electrodes in the semiconductor detector. The collection time is also spread out because of the diffusion. One can often neglect the consequence of diffusion, but for large volume detectors or when position or timing measurements of high precision are involved it must be taken into account.

The Silicon detectors that are used in the experiments that this thesis is about are so called Silicon diode detectors. As the name implies the detector consists of a diode. When two differently doped, n and p, regions of silicon are into contact with each other a np diode is formed. It is the junction between the the two doped regions that are important for detections of charged particles. If a tension is applied in the reverse direction a depletion zone is established where no charge carriers are present. When a charged particle enters this depleted zone it will create electron hole pairs which then will be collected because of

the applied tension and it is this current of electron hole pairs that makes up the signal from the detector.
Gas detectors works in a similar way with the difference that ionisation of the gas requires about 10 times more energy than to create an electron hole pair. Because of this semiconductor detectors have about 10 times more charge carriers than gas detectors for the same incoming particle. This gives the silicon detector a smaller statistical fluctuation which helps to improve the limiting energy resolution. Besides, already mentioned, that the semiconducting detectors are small in size and give a fast response, semiconductor detectors have a better stopping power on the incoming particles because of its high density.

Chapter 3

Electronics and radiation sources

As with all experimental physics, a lot of electronics are needed for acquiring data from experiments. This section contains information of the electronics and radiation sources used in the experiments.

3.1 Silicon detectors

Different types of semiconducting silicon detectors were used for different radiation sources. The first detector used to measure radiation from the α products (see table 3.1 in subchapter *Radiation sources*) was an *Enertec Schlumberger model* $IPE\ 150-500.14.TM$, 4716. This detector has an active area of $150mm^2$, its thickness is $500\mu m$ and its energy resolution is $14keV$ for $5.5MeV\alpha$ particles. The maximum tension over this detector is $40V$. Later on this detector was replaced by another Si-detector, also an *Enertec Schlumberger*, but model IPW 20.250.10, $S018$. The active area of this detector is $20mm^2$, its thickness is $250\mu m$ and its energy resolution is $10keV$ for $5.5MeV\alpha$ particles. The recommended maximum tension for the Si-detector is $120V$, but due to an inner resistance in the preamplifier it is possible to excess this limit without damaging it. A higher tension is a good thing to have since it increases the depletion zone in the detector and thus the sensitive volume for radiation detection. High tension is also needed for a fast collection of radiation ionised electrons.

While using the first detector, both its sides are used for particle detection (i.e. the detector is placed (and used) with the particle injection from both front and rear side. Figures 3.1*a* and *b* shows the front and rear side of such a detector.

The second detector was also used when detecting radiation from a fission source (α and different fission products), see table 3.2 in subchapter *Radiation sources* below.

(a) Front side (b) Rear side

Figure 3.1: Both sides (i.e. with the particle injection from both front and rear side) of a Si-detector can be used for detecting incoming radiation. To the left (a) the front side of the Si-detector is seen and to the right (b) the rear side. The detector model seen in the figures is an *Enertec Schlumberger, model IPW* 20.250.10, *S*018.

3.2 Radiation sources

Naturally occurring sources are elements that through nuclear decay emits e.g. α, β and/or γ radiation. Some heavier nuclei, e.g. uranium, emits heavy, charged particles through fission reactions. For the experiments it would be optimal to have as many different, charged particles as possible for the PSD analysis when calculating on particles with energies below $2MeV/nucleon$ which is why a particle accelerator is to prefer.

The lack of an accelerator at *Chalmers* leads to the use of other radiation sources. The α source used in the experiments actually consists of three α sources that emits particles with different energies. The elements are: $Pu-239$, $Am-241$ and $Cm-244$, [11]. See table 3.1.

Table 3.1: Three different types of α source.

Source (single α emitter)	$t_{1/2}$ y	E_α MeV	% Branching
^{239}Pu	$2.41 \cdot 10^4$	5.1554	73
^{241}Am	433	5.48574	85.2
^{244}Cm	18.11	5.80496	76.7

The fission source is $Cf-252$ (Californium). $Cf-252$ is an unstable nucleus decaying into α and different fission products, see Table 3.2.

Table 3.2: The fission source is ^{252}Cf. Since there are several decay modes for ^{252}Cf the energies for its fission products are not tabulated.

Source	$t_{1/2}$ y	E_α MeV	% Branching (α)	% Branching (other fission products)
^{252}Cf	2.645	6.21687	96.908	3.092

3.3 Preamplifiers

For the test setup an *EG&G Ortec* 142*A preamplifier* [13], seen in figure 3.2, is used. It is a charge-sensitive unit used for room-temperature-operated silicon surface-barrier detectors. It has an input capacitance range from $0 - 100pF$ and gives both an energy output and time output signal. A disadvantage with this preamplifier is that it does not collect the charges from the detector fast enough which leads to an incorrect pulse shape (e.g. affects rise time calculations). Therefore another, faster preamplifier is used for the real setup. The latter is a charge-sensitive, modified (i.e. tuned for heavy ions) $CSTA2$ dual preamplifier [5][14]. It provides a slow energy output and a fast timing output, see figure 3.3. The gain for the $CSTA2$ is adjustable via an internal screw (coarse adjustment) for α particles or heavy ions. There are also two external screw controls, one for fine gain and the other for DC level adjustments. This model is built by the electronic laboratory of the *Institute of Nuclear Physics*, *University of Technology*, *Darmstadt* (TUD).

Figure 3.2: *EG&G Ortec* 142*A* preamplifier

3.4 Vacuum pumps and vacuum chamber

To minimise the detection and interference of electromagnetic radiation, causing unwanted noise, the detector is placed in a vacuum chamber. Two different types of vacuum pumps are used. The first one (primary pump) is a $Varian\ SH-100$ *Dry scroll single hermetic vacuum pump*. It is used to lower the atmospheric pressure in the vacuum chamber to about $5 \cdot 10^{-1}$ $mBar$. At this pressure a second pump, a $Varian\ Turbo\ V301$ *vacuum*

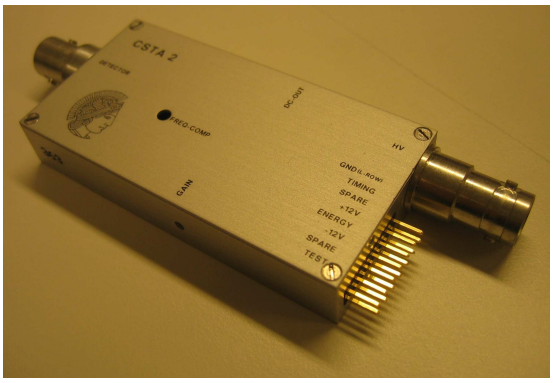

Figure 3.3: Modified (tuned for heavy ions) $CSTA2$ preamplifier.

pump, starts pumping and further reduces the pressure to about $5.5 - 6.0 \cdot 10^{-7}$ $mBar$. The vacuum chamber is a home made (at Chalmers) aluminium chamber with the size $60x44.5x51$ cm (LxWxH). A $Varian$ $senTorr$ $gauge$ $controller$ are used as pressure controlling device. Detector and radiation source is placed inside the chamber and the signal cables from the detector are connected with outside equipment through conductor joints at one side of the vacuum chamber. The complete vacuum system setup with chamber, pumps and controlling device is seen in the following figure (fig. 3.4).

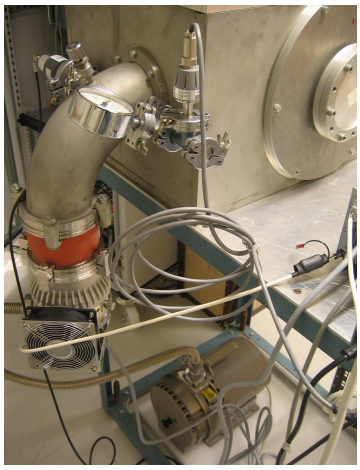

Figure 3.4: By putting radiation source and detector in an evacuated environment (i.e. vacuum) detected noise, generated by electromagnetic radiation and/or the interaction between atmospheric and radiation particles before arriving to the detector, is reduced to a minimum. Controlling and powering devices are seen left to the chamber and the primary pump is seen on the floor under the table. The secondary pump is placed behind the chamber.

3.5 Power supplies

The primary vacuum pump ($Varian\ SH-100$) is connected to the national power grid while the secondary pump ($Varian\ Turbo\ V301$) has its own power supply. The $DC-power\ supplies$ for the detector and preamplifier's are of NIM-standard. For the Si-detector a $Canberra\ CM\ 3122D\ HV\ power\ supply$ [15] is used. It has a voltage range from $0-\pm\ 1200VDC/0-\pm\ 120VDC$ and current range from $0-300\mu A$. Its amplification up and down is linear and it has a $2\mu A/20\mu A$ full scale selectable range and positive and negative output polarity option. An $Ortec\ 460\ Delay\ line\ amplifier$ generates $\pm 12V$ for the preamplifier.

3.6 Oscilloscope

The oscilloscope, used for collecting the preamplified analogous signals from the silicon detectors, is a $Lecroy\ WavePro\ 7000A\ digital\ oscilloscope$ [16], figure 3.5 below. This device has an installed version of WinXP operating system and an built in 20 GB hard drive which makes it more than just an oscilloscope. It works also as a computer and can be used to analyse detected signals. The $WavePro\ 7000A$ has four input channels, a $1GHz$ bandwidth capacity and a sampling frequency of $20GS/s$ in dual mode ($10GS/s$ in quad mode). The typical rise time for this device is $400ps$ which is fast enough not to affect the rise time of the incoming signals. This is essential since a distortion in the signal contributes to information loss.

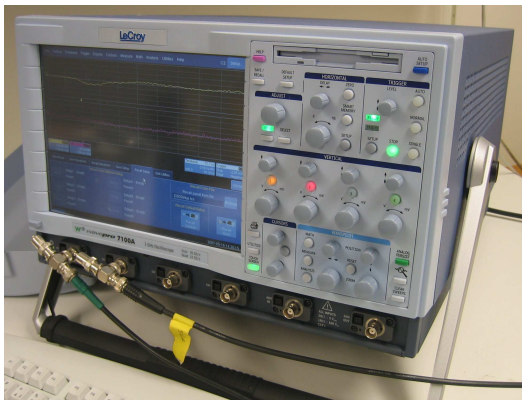

Figure 3.5: A $Lecroy\ WavePro\ 7000A\ digital\ oscilloscope$ is used to collect amplified signals from the silicon detector.

Chapter 4

Data-analysing programs

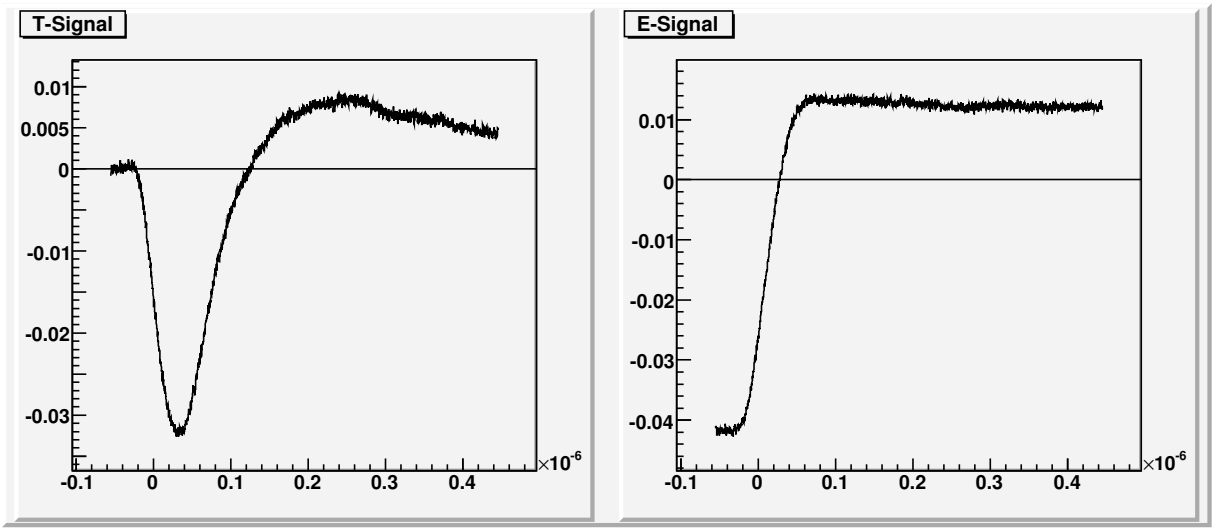

Figure 4.1: T-Signal and E-Signal

Two kinds of pulses are obtained from the preamplifier, a T-signal and E-signal (see Figure 4.1). The T-signal is the fastest of the two pulses and are generally used for various timing electronics. For the purpose of PSD, this signal is interesting because it should contain a more precise rise time than the E-signal. The E-signal however is used to measure the energy of the detected particle but some information is lost in the process of producing it, which gives this signal a less precise rise time.

Analysing the pulse, i.e calculating the rise time and amplitude, is done in 4 steps.

- Load the pulse.
- Smooth the pulse to remove noise.
- Find the baselines of the pulse.
- Calculate the rise time or amplitude depending on the type of the loaded pulse.

Loading the pulse is simple as the oscilloscope saves the data as ASCII-files. In the case of a negative T-Signal the pulse is flipped around the horizontal axis becuase a positive signal is needed to calculate the rise time.

To reduce noise a simple filter algorithm is applied to the data, also known as a Box smoothing algorithm. The idea is to take an average over M points before and after the i:th point. This average replaces the value in the i:th point and the process is repeated over all data points. The formula for this is as follows:

$$Y_i = \left(\sum_{j=i-M}^{i+M} Y_j \right) / \left(2 \cdot M + 1\right) \tag{4.1}$$

This algorithm makes the curve smoother and removes the worst part of the high-frequent noise in the signal. The amount of smoothing depends only on the value of M. A high M value means that the average is calculated over a large amount of data points which results in a high smoothening effect and vice versa. Too much smoothening can distort the pulse to the point where later calculations might be incorrect. Empirical studies shows that the number of data points divided by 200 is generally a good value for M. In Figures 4.3 and 4.2 an example of how the smoothening effect will look can be seen.

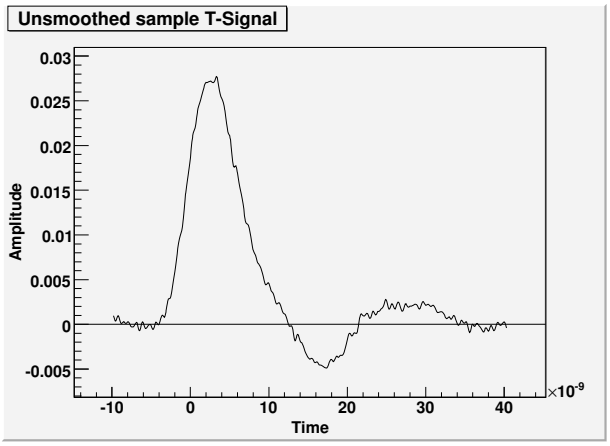

Figure 4.2: An example of an unsmoothed pulse

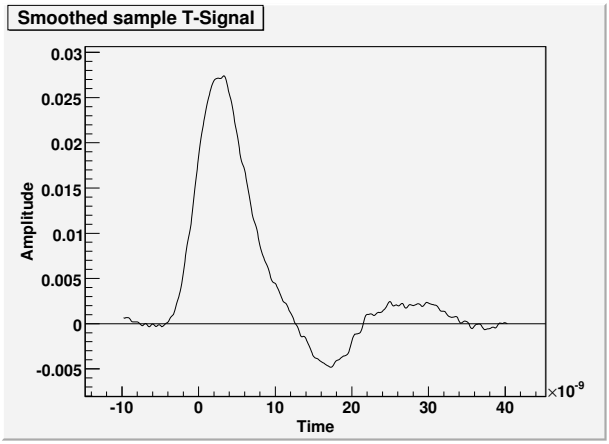

Figure 4.3: An example of a smoothed pulse

After the signal has been smoothed the next step in the analysis is to find the baselines of the pulse. Baselines are defined as when the signal have a slope that is zero. To find the baselines the pulse is divided into a number of segments for which the mean value and RMS is calculated. By taking the difference between the mean value for two neighbouring segments one gets a number of values for each pulse, representing in a crude way the slope of the pulse. Figure 4.4 gives an example of how the values vary with the slope of the pulse. As can be seen the values will be very small if the slope of the pulse is close to zero for two neighbouring segments and if there is an upward or downward slope the value will be non zero.

To ease further calculations these values are normalised by dividing with the largest value and all negative values are negated so as only positive values are obtained. As stated before a baseline is defined as when the slope for the pulse is zero and to decide how low of a value is needed for the segments to be counted as a baseline a threshold is calculated. This threshold is determined by taking an average of all the values except those above 0.5.

A lot of baselines will be found but there is only need for two, or one in the case of a T-signal, to do all the calculations and hence the baselines need to be sorted. That is why also the RMS is calculated for each value so that the value with the least amount of error of all similar values can be selected.

When the baselines have been calculated all there is left is to calculate the amplitude and rise time which is a quite simple procedure. The amplitude of a pulse is given just by the difference between the highest and lowest baseline.

Rise time is calculated by first finding the two data points that are closest to 10 and 90 percent of the pulse amplitude and a linear fit is made around these points to get a value with more decimals. By taking the difference between the corresponding X-positions (10 and 90 percent) the rise time is calculated.

These algorithms are implemented using the C++ library ROOT developed by CERN and

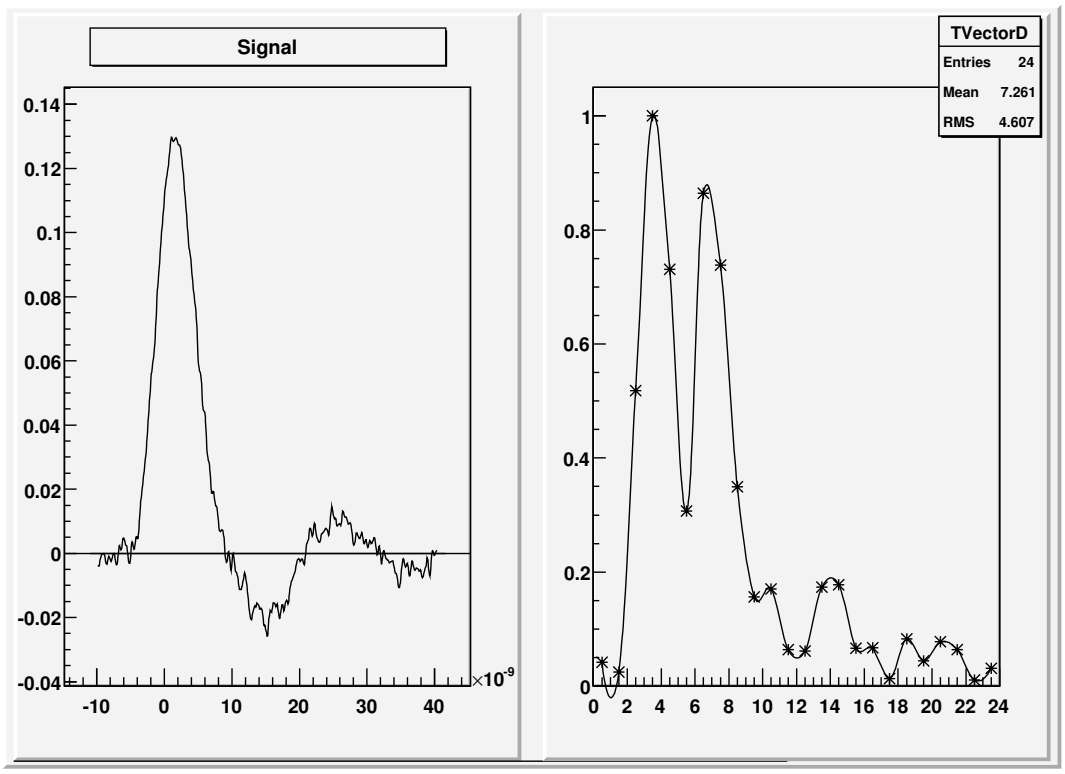

Figure 4.4: The right sub figure shows how the values to determine baselines vary with the slope of the pulse in the left sub figure.

the standard GNU C++ Compiler. All the algorithms and functions are contained in a class which makes the program easy to use and customise. With the help of some standard C libraries the program can be made to go through a large amount of data files, calculating amplitudes and rise times for each file. The data will then be stored as a NTuple class in a file which uses a file system developed by ROOT. This makes the data easy to access through ROOT's built in C++ interpreter, which is capable of drawing histograms, scatter plots etc.

Chapter 5

Experiment

To see if there is a possibility to separate charged particles from each other with PSD some experiments have to be made. Our first experimental studies were made at Chalmers, Gothenburg. There we got acquainted with the experimental setup and procedures and learnt to solve problems before we had the opportunity to take part in an experiment at Centro Nacional de Acceleradores, CNA, in Seville, Spain, where an experiment with an aim similar to our thesis work was executed.

5.1 Gothenburg experiments

Here follows a description of our experiments at Chalmers, Gothenburg. The electronics mentioned in this section is the described ones in Chapter 3.

5.1.1 Experimental setup

The radiation source and silicon detector are placed inside the vacuum chamber, this is to avoid detection of other particles in the atmosphere and air scattered radiation particles. The signal cable from the detector is connected with outside equipment via conductor joints at one side of the vacuum chamber. A preamplifier is connected to the outside signal cable. The first amplifier used was a *EG & G Ortec* preamplifier. Since this one is too slow for charge collection, affecting detected rise-time, another faster amplifier is used (a $CSTA2$). NIM-standard power supplies are powering detector and preamplifier. Coaxial cables connect the amplifier's time and energy output with the input channels on the oscilloscope. The digital oscilloscope collects and stores (ASCII format) incoming data. The information is then transfered to a computer for further analysis.

5.1.2 Procedure

During the first test period, pure α-sources consisting of ^{239}Pu, ^{241}Am and ^{244}Cm were used. These sources are later exchanged by a fission source, also generating α. The latter

source gives the ability to detect particles with different total energy (α and other fission products) at the same time giving the possibility to see differences in e.g. rise time.

Radiation source and Si-detector are placed inside the vacuum chamber, separated by a short distance of about five centimetres. The silicon detector is firstly placed with the particle injection coming from the front side. Later on this is changed to the rear side, which is supposed to give better results but for some reason this did not work at all and only the front side of the detector is used. A signal cable from the the detector is connected to a connection joint in the wall and there after the chamber is sealed. The vacuum pumps are activated and after achieving sufficiently high vacuum the power supplies for the silicon detector and preamplifier are switched on. The tension over the detector depends on the type of detector, for the *Enertec Schlumberger IPW* 20.250.10, $S018$, $140V$ is applied. From the time (T) and energy (E) outputs of the preamplifier coaxial cables are connected to the Lecroy digital oscilloscope, where the signals are collected and stored. When a particle hits the detector two coincident signals are collected from the T and E outputs which makes it possible comparing rise time from the T output and amplitude from the E output of the signal. The triggering function in the oscilloscope is set to trigger on the time signal. When doing so radiation generated pulses from the detector are captured and saved in $ASCII$ format on its internal hard drive.

The stored information is transfered to a computer where it is analysed with the algorithms explained in chapter 4. Matlab is also used to plot some data which could not be plotted in an easy way with ROOT.

5.2 Seville experiments

These experiments took place the 5-9 of February 2007 at CNA by a Spanish group from the University of Huelva and an Italian group. The aim of the experiment was to test different electronic circuits like AD-converter, preamplifier and detectors and to optimise these for future applications. A method is sought to identify different particle energies, masses and charge by analysing the shape of the pulse, like our thesis is dealing with.

5.2.1 Experimental setup

CNA in Seville has an ion source connected to a tandem accelerator that can generate a maximum tension of $3MV$. A dipole deflection magnet deflects the beam in to the correct angle and works also as a mass separator, extracting the desired, ionised isotope. The beam hits a thin metal foil that deflects the beam through elastic scattering to decrease the intensity of the beam, avoiding any destruction of the detector.

The scattered beam hits the detector which is connected to a preamplifier and other electronics (some are NIM-standard) like power supply, AD-converter, oscilloscope (LeCroy WavePro 7000 A Series) and computer. The beam and target are placed inside a vacuum chamber, see Figure 5.1.

The detector used was a neutron doped silicon detector. The fast preamplifier was Italian made.

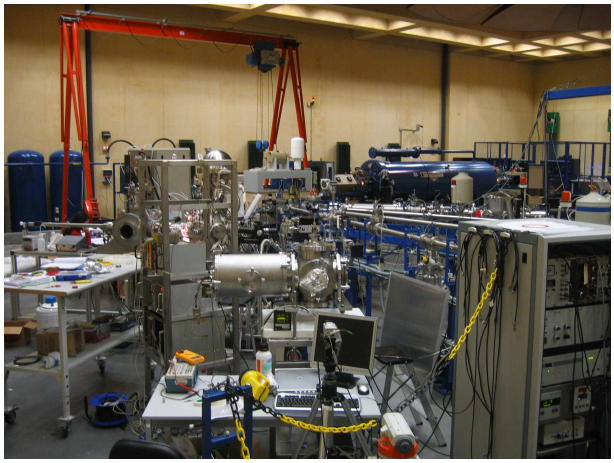

Figure 5.1: Parts of the experimental setup in Seville with the vacuum chamber containing the detector in the fore ground.

5.2.2 Procedure

The ion source and electronics were tuned for optimal performance and for noise reduction a lot of aluminium foil was used as shield for electromagnetic radiation. Several different types of ions were produced in the ion source and accelerated towards the detector after being deflected and collimated. The ions used were: p, d, α, ^{6}Li, ^{7}Li and ^{12}C. By varying the tension of the accelerator different particle energies were obtained, from $4MeV$ to $12MeV$, for each isotope. The obtained signals were collected and stored in an oscilloscope and transfered to a computer for analysis.

Chapter 6

Results and discussion

The results from our experiments are presented here in two sections for the two experiments we made. Discussion of the results are included in the text.

6.1 Seville experiment

The data from the Seville experiments were run through the data analysing programs where rise time and amplitude were calculated. The rise times and amplitudes for the different particles were plotted against each other in individual scatter plots, see Figures 6.1, 6.2. As can be seen in the scatter plots the results are a bit inconclusive. In e.g. the ^{4}He scatter plots there is a good definition of rise time whereas in the ^{6}Li scatter plots there is a large spread of rise times. An example of the spread of rise time in the ^{6}Li scatter plots are shown in figure 6.3 We think that this spread is due to changes in the experimental setup during the experiment, e.g. change in amplification, beam profile or noise changes. Because of this we can not see any separation of the charged particles.

This is not the result we were expecting to get since, as have been stated before in this report, we where expecting to see that the rise times for ^{6}Li would be faster than for ^{4}He and this is obviously not the case. There may be many reasons to the inconclusive results such as: inelastic scattering, problems with the beam, electronic issues and other unknowns.

Because the beam profile is unknown we think the beam has struck an obstacle, like the edge of the collimator, resulting in an inelastic scattering. Figure 6.4 shows a histogram of the amplitude (and hence the energy) for the data set of ^{7}Li at 8 MeV. The two peaks in the histogram might show that there is inelastic scattering. Some of the data shows tendencies towards the rise time dependence we where looking for but it can not be stated for sure that this is the fact since the data is so inconclusive.

In some data, however, we can see tendencies of charged particle separation like ^{6}Li and ^{7}Li, see Figure 6.5. But these trends are too vague for us to present any facts of us succeeding in identifying different charged particles from each other.

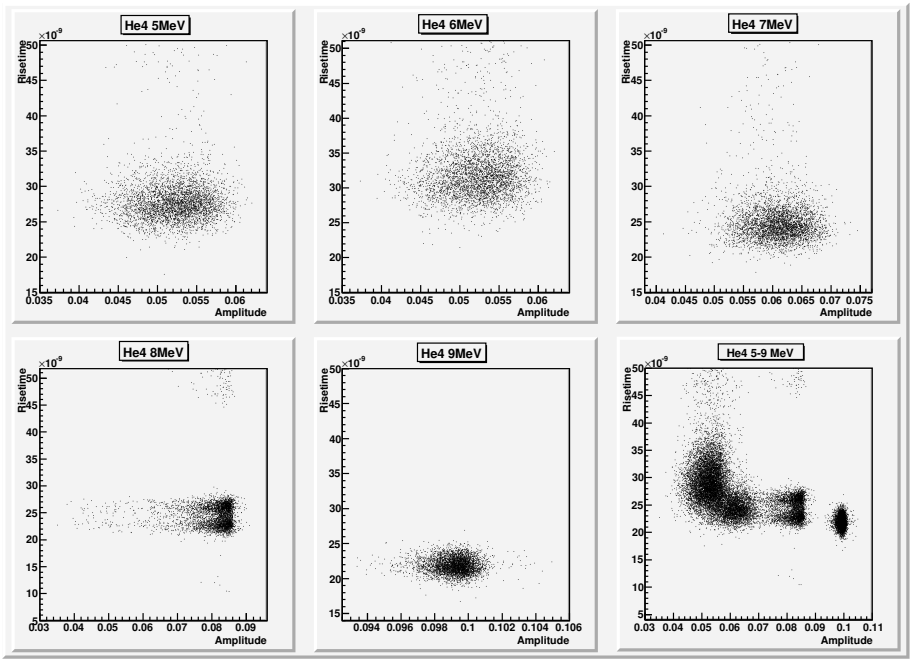

Figure 6.1: Scatter plots for different energies of ^{4}He

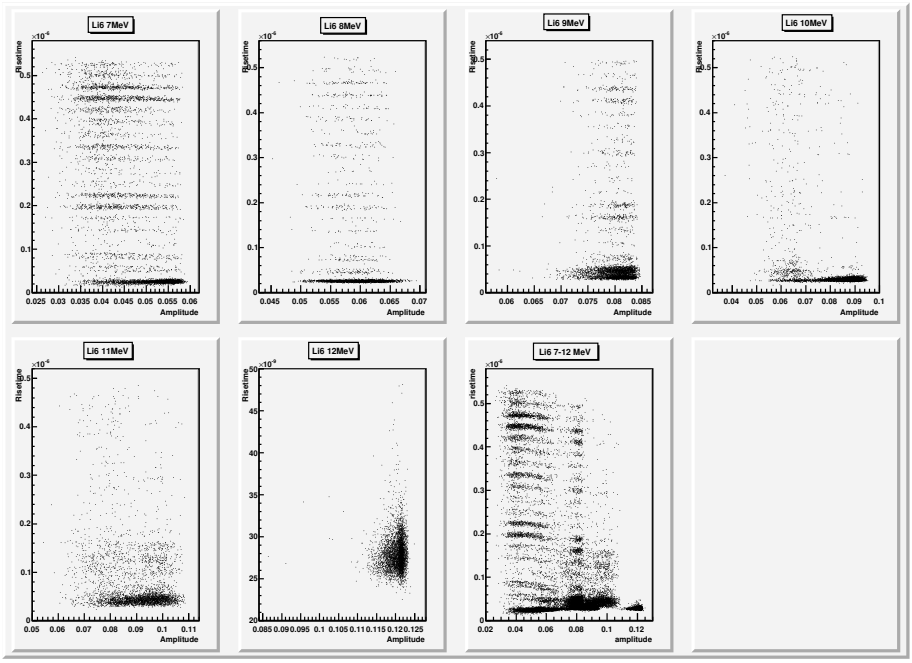

Figure 6.2: Scatter plots for different energies of ^{6}Li

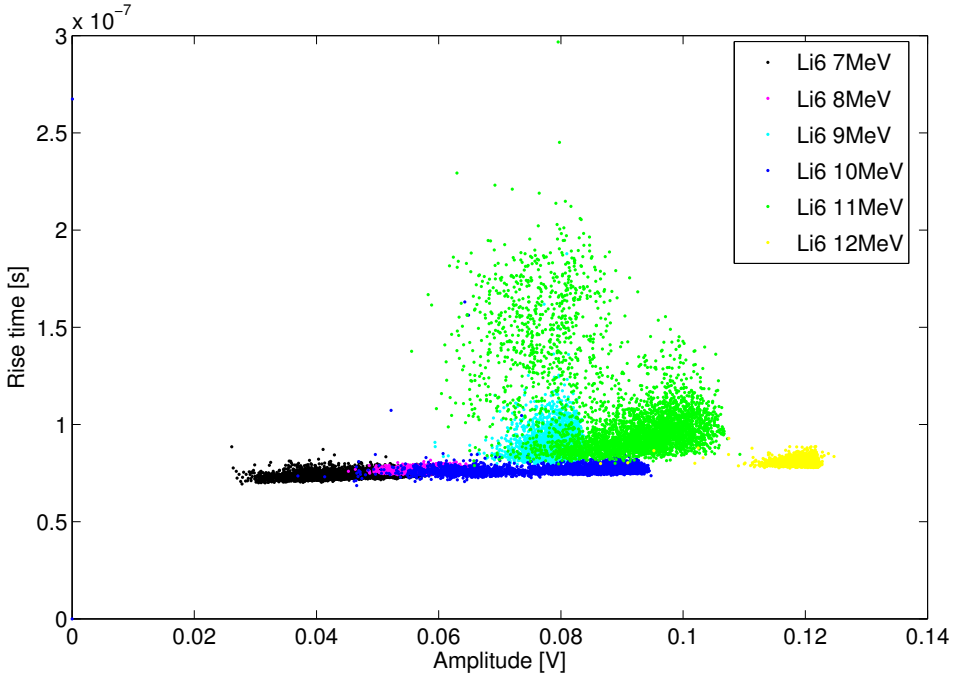

Figure 6.3: Scatter plot of ^{6}Li at different energies.

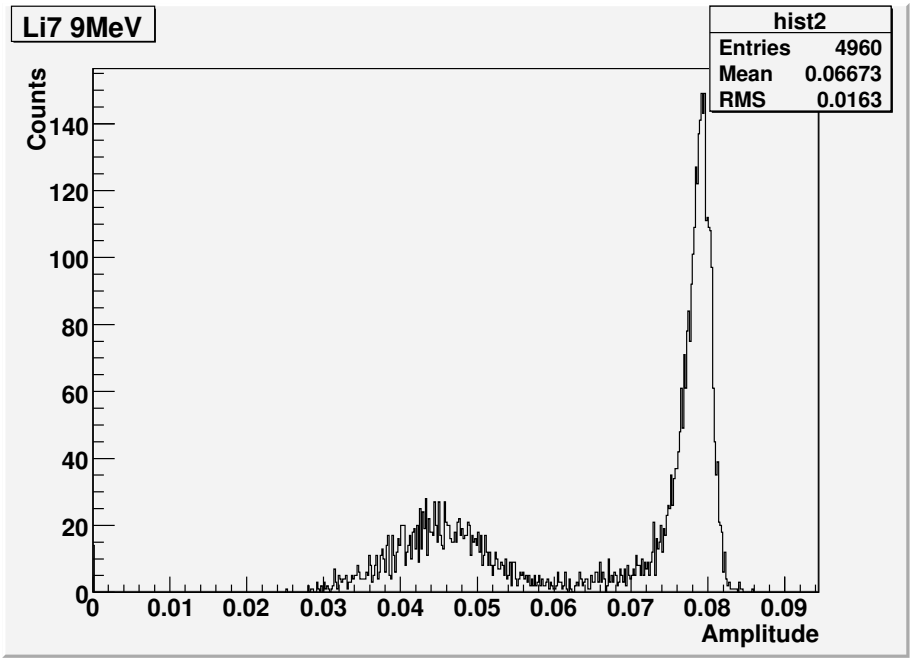

Figure 6.4: Histogram over amplitude for ^{7}Li 9MeV

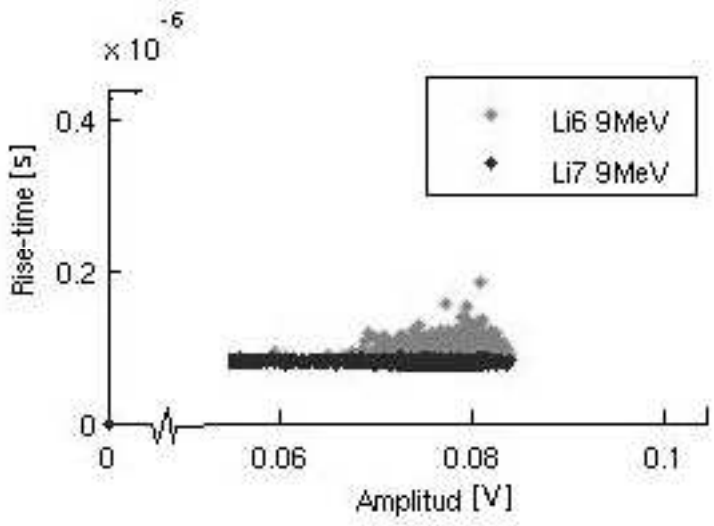

Figure 6.5: A scatter plot of rise time versus amplitude for ^{6}Li and ^{7}Li at $9MeV$. A tendency of separation can be seen between these isotopes.

6.2 Gothenburg experiment

Due to the limitation in charged particles to experiment with we were only able to save the pulses from α particles and fission products from ^{252}Cf for analysis. What we found was not what we expected, running the data through our programs gave us a rise time for α particles faster than the rise time for the fission products, which is contradictory to what we stated earlier in this thesis. However this seems to be right as comparing rise times directly in the oscilloscope gives rise times which is the same as the algorithms give us, which points to a electronic problem. Since the signals from the fission products are much stronger than signals from the α particles the preamplifier might have a problem with the large difference in signal strength. We also wanted to take data from a beta emitting source but because of some problems and lack of time we did not get any data from fast electrons. Because of this and the fact that there was no difference in rise time between α particles and fission products we did not get any good results. However in Figure 6.6 one can see a scatter plot from the α source with its three different energies.

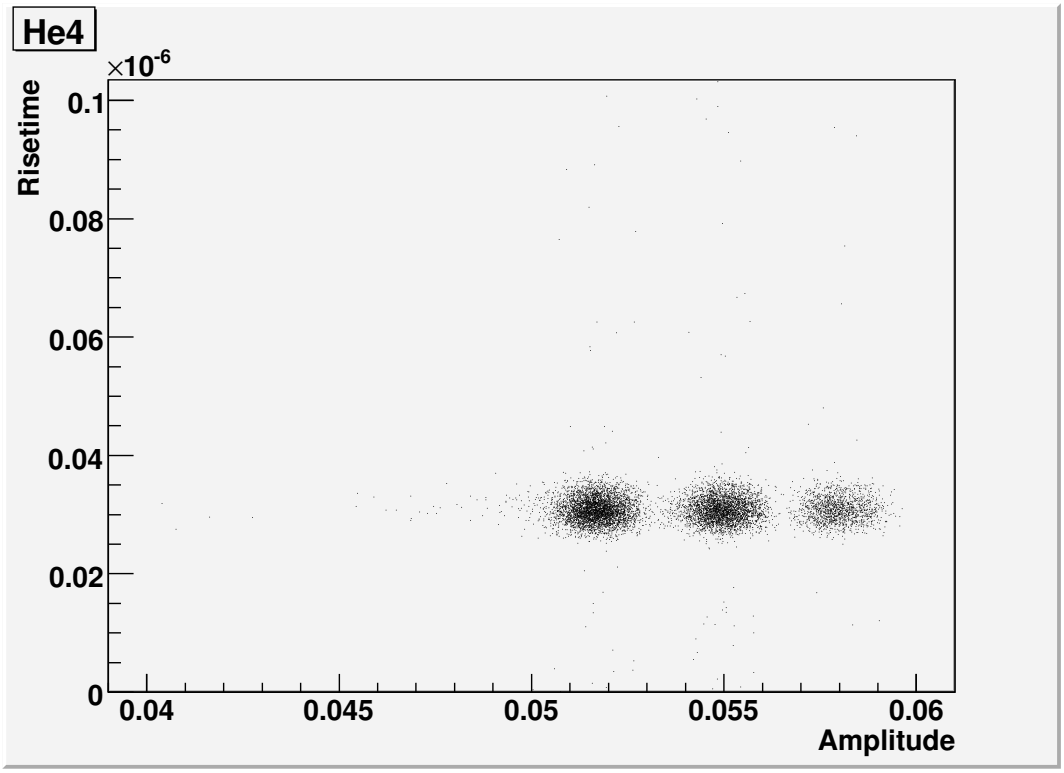

Figure 6.6: A scatter plot of rise time versus amplitude for ^{4}He for the α source described in chapter 5.

Chapter 7

Conclusion and outlook

Looking at our results we conclude that with our experimental results we can not separate charged particles as we hoped. With better experimental data we might be able to prove that the tendencies we saw actually were separation of particles, but it is hard to speculate in these issues. It might also be that the algorithms used in calculating rise times and amplitudes might not be accurate enough to be able to give a correct result. A big problem is that no one else that we know of also can analyse the data.

If we were to continue this project and could do more experiments we would like to do an experiment like we did in Seville again, but with improvements such as better control over the beam profile, electronics etc. Such an experiment is planned to be done in Madrid sometime in the near future. Hopefully there will be some better data to analyse then.

An other approach than to directly compare rise times might be to utilise an artificial neural network, i.e. a set of computer algorithms that mimic a biological neural network. A neural network has the ability to learn how to distinguish different patterns from each other and are mostly very efficient in doing so. Artificial neural networks are very complicated and time consuming to develop so unfortunately there was not enough time to look into this possibility for out thesis. However this might be a promising future method of separating particles from each other.

If discrimination of particles could be achieved it will be a very important method in nuclear experiments. It will probably not be the only type of method to identify particles since ΔE-E setups work really well however at low energies ΔE-E do not work, because particles are stopped in the first thin detector. Although many experiments usually have particles of high energy there is some experiments that need to detect and identify particles with very low energy. That is why it would be really interesting to develop PSD, especially for these low energy experiments.

Bibliography

[1] W. R. Leo, *Techniques for Nuclear and Particle Physics Experiments - Second Edition* (Springer-Verlag, New York Berlin Heidelberg 1994) Chapters 2, 10

[2] Glenn F. Knoll, *Radiation Detection and Measurement - Third Edition* (John Wiley and Sons, Inc. 2000) Chapters 2, 11

[3] Kenneth S. Krane, *Introductory Nuclear Physics* (John Wiley and Sons, Inc. 1988) Chapter 7

[4] Charles Kittel, *Introduction to Solid State Physics - Seventh Edition* (John Wiley and Sons, Inc., 1996) 221-226

[5] M. Mutterer et al., *IEEE Trans. Nucl. Science 47 (2000) 756*

[6] G. Pausch et al., *IEEE Trans. Nucl. Science 43 (1996) 1097*

[7] G. Pausch et al., *IEEE Trans. Nucl. Science 44 (1997) 1040*

[8] J. Lu et al., *Nucl. Instr. and Meth. A 471 (2001) 374*

[9] B. K. Nayak et al., *Pramana 65 (2005) 1053*

[10] M. Alderighi et al., *Nucl. Phys. A 734 (2004) E-88*

[11] Edgardo Browne, Janis M. Dairiki and Raymond E. Doebler, *Table of isotopes - Seventh edition* (John Wiley and Sons, Inc. 1978) Appendices p.7

[12] Richard B. Firestone and Virginia S. Shirley, *Table of isotopes - Eighth edition, volume 2* (John Wiley and Sons, Inc. 1996) p.2857

[13] EG&G Ortec, *Models 142A, 142B and 142C preamplifier operating and service manual* (Printed in U.S.A., EG&G Ortec Part no. 627990)

[14] Radomira Lozeva, *A new developed calorimeter telescope for identification of relativistic heavy ion reaction channels* (University of Sofia "St. Kliment Ohridski", Faculty of physics, april 2005) p.34-35

[15] Canberra Elektronik Gmbh, *Model 3122D high voltage power supply - operator's manual* (Canberra Elektronik Gmbh)

[16] LeCroy, *WaveMaster series, WavePro 7000A series, DDA series, SDA series operator's manual* (LeCroy Corporation 2005)